Chiral Nanostructures

Deutsche Ausgabe: DOI: 10.1002/ange.201608638
Internationale Ausgabe: DOI: 10.1002/anie.201608638

Role of Achiral Nucleobases in Multicomponent Chiral Self-Assembly: Purine-Triggered Helix and Chirality Transfer

Ming Deng, Li Zhang, Yuqian Jiang, and Minghua Liu**

Abstract: *Chiral self-assembly is a basic process in biological systems, where many chiral biomolecules such as amino acids and sugars play important roles. Achiral nucleobases usually covalently bond to saccharides and play a significant role in the formation of the double helix structure. However, it remains unclear how the achiral nucleobases can function in chiral self-assembly without the sugar modification. Herein, we have clarified that purine nucleobases could trigger N-(9-fluorenylmethox-ycarbonyl) (Fmoc)-protected glutamic acid to self-assemble into helical nanostructures. Moreover, the helical nanostructure could serve as a matrix and transfer the chirality to an achiral fluorescence probe, thioflavin T (ThT). Upon chirality transfer, the ThT showed not only supramolecular chirality but also circular polarized fluorescence (CPL). Without the nucleobase, the self-assembly processes cannot happen, thus providing an example where achiral molecules played an essential role in the expression and transfer of the chirality.*

Helical nanostructures, such as α helices in proteins, double-helical deoxyribonucleic acid (DNA), and the triple helix in collagen, are beautiful and widely observed in biological systems. These helical nanostructures play an important role in the construction of three-dimensional architectures to express unique biological functions.[1] As a result of evolution, nature utilizes saccharides, amino acids, and nucleobases as the fundamental building blocks for the creation of biomacromolecules as well as the chiral self-assembly into well-organized nanostructures.[2] Both amino acids and saccharides are major chiral units that form the biomacromolecules through the covalent bonds and then fold into three-dimensional structures through non-covalent bonds. Achiral nucleobases utilize their H-bonding capacity to support DNA double-helix structures, which means that the role of achiral molecules is also very important for understanding the origins of chirality in supramolecular systems. In mimicking the biological chiral self-assembly, amino acids, peptides, and saccharides have been extensively investigated,[3] while self-assemblies containing achiral nucleobases are relatively less studied. As an important achiral component, nucleobases usually covalently bond to sugar and play a significant role in the formation of the double-helix structure. However, it remains unclear how the achiral nucleobases can function in the chiral self-assembly without modification by the saccharides.[4] Herein, we have investigated self-assembly based on a chiral amino acid, achiral nucleobase, and dye, in order to understand the role of the achiral molecules in multicomponent chiral self-assemblies. We have unexpectedly found that the achiral nucleobase can trigger the helix of Fmoc-Glu and transfer their chiral sense to the achiral cationic dye. Figure 1 illustrates the helical structures formed by Fmoc-Glu with achiral purine nucleobases (guanine (G) or adenine (A)). In addition, when a fluorescent molecule is introduced into the two-component assemblies, it will also express helicity at the nanoscale level and further transfer the chirality to the fluorescent molecules, thus leading to a strong circular-polarized fluorescence (CPL). In the absence of A or G, Fmoc-Glu will not express the chirality. And the chirality of Fmoc-Glu cannot be directly transferred to ThT without the aid of nucleobase, indicating that achiral nucleobases play an essential role in the expression and transfer of chirality.

The self-assemblies of Fmoc-Glu (L or D enantiomers) together with nucleobase were performed in aqueous solution. A racemic mixture of Fmoc-Glu was not used in this study. Fmoc-Glu (L or D) itself cannot self-assemble into hydrogels, but upon mixing with the nucleobase, hydrogels or precipitates are formed depending on the structure of nucleobase. Purines (G or A) were found to form an opaque and translucent hydrogel with Fmoc-L-Glu, respectively. In contrast, no hydrogels were presented in the pyrimidine nucleobase (thymine (T) or cytosine (C)), as shown in Figure S1. Rheological studies further revealed hydrogel formation of Fmoc-Glu with purine nucleobases (Figure S2). The storage modulus (G′) was found to be approximately an order of magnitude larger than the loss modulus (G″), indicative of an elastic rather than viscous material. Such rheological behavior is characteristic of gel materials.[5]

[*] M. Deng, Dr. L. Zhang, Prof. Dr. M. Liu
Beijing National Laboratory for Molecular Sciences
CAS Key Laboratory of Colloid Interface and
Chemical Thermodynamics Institute of Chemistry
Chinese Academy of Sciences
Beijing, 100190 (P.R. China)
E-mail: zhangli@iccas.ac.cn
liumh@iccas.ac.cn
M. Deng, Prof. Dr. M. Liu
University of Chinese Academy of Sciences
Beijing, 100049 (P.R. China)
Dr. Y. Jiang, Prof. Dr. M. Liu
Laboratory for Nanosystem and Hierarchy Fabrication
CAS Center for Excellence in Nanoscience
National Center for Nanoscience and Technology
Beijing 100190 (P.R. China)
Prof. Dr. M. Liu
Collaborative Innovation Center of Chemical Science and Engineering, Tianjin, 300072 (P.R. China)

Supporting information for this article can be found under: http://dx.doi.org/10.1002/anie.201608638.

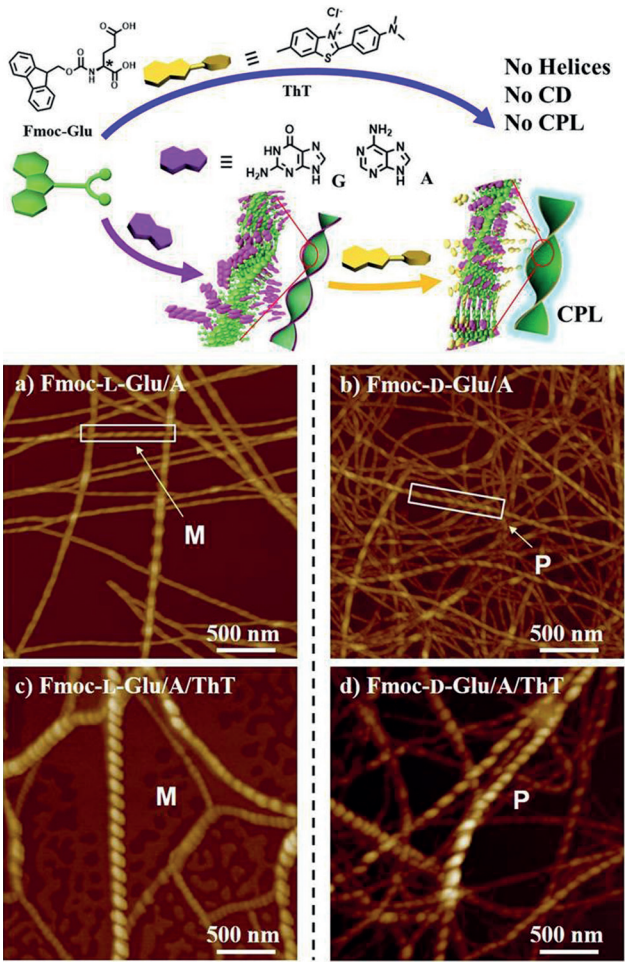

Figure 1. Top: Chemical structures of the Fmoc-Glu, purine nucleobase, and achiral dye (ThT), and illustration on the achiral purine-nucleobase-mediated chirality transfer from Fmoc-Glu to achiral ThT. Fmoc-Glu and purine nucleobase self-assemble into helical structures. Upon further mixing with ThT, they further self-assemble into helices. In the absence of A or G, no assembly or chiral nanostructures are obtained. Bottom: a, b) AFM images of Fmoc-L(D)-Glu/A; c, d) AFM images of Fmoc-L(D)-Glu/A/ThT self-assemblies.

The nanostructures obtained in hydrogels can be visualized by AFM and SEM (Figures 1, S3, and S7). Figure 1 a,b shows helical nanostructures formed in the complex of Fmoc-Glu/A. Left-handed helices appear in the co-hydrogel of Fmoc-L-Glu and A (Figure 1 a). The height profile of fibers obtained from AFM images analyzed by NanoScope Analysis or statistical analysis by software FiberApp[6] revealed that these helices have a pitch of around 125 nm and width of about 90 nm. By contrast, right-handed helices were found when Fmoc-D-Glu is used. The mirror image of the helix indicates that helicity is determined by chiral information of Fmoc-Glu. SEM was further utilized to confirm the morphology and nanostructures of Fmoc-Glu with four nucleobases. Fmoc-Glu (L and D) exhibited irregular nanostructures (Figure S3a). Addition of A or G caused the emergence of helical nanostructures (Figure S3b, b′, e, e′). Mirror images of the helices were found to be induced by the enantiomer of Fmoc-Glu, further indicating that molecular chirality of Fmoc-Glu could be transferred to the macroscopic level and control the chirality of the nanostructures.[7] Pyrimidine nucleobases C or T cannot trigger Fmoc-Glu to build any chiral structures. In the case of T, short but wide ribbons with width of about 300 nm form (Figure S3c,c′), which are significantly larger than that of Fmoc-Glu/A (G). Addition of C caused a greater difference than that of Fmoc-Glu/A (G). Microflowers composed of nanoflakes were obtained (Figure S3d,d′). The common morphological features between Fmoc-Glu/C and Fmoc-Glu/T are the absence of chiral sense and nanostructures with larger size, which lead to precipitation (Figure S1d,e).

Circular dichroism (CD) spectroscopy is a powerful tool for understanding the arrangement of chiral molecules in the associated state because intermolecular interactions, especially between chromophore molecules, may produce striking chiroptical responses and generate CD signals often much stronger in the associated state compared to their isolated molecular state. Figure 2 and Figure S4 show the CD spectra of the gels.

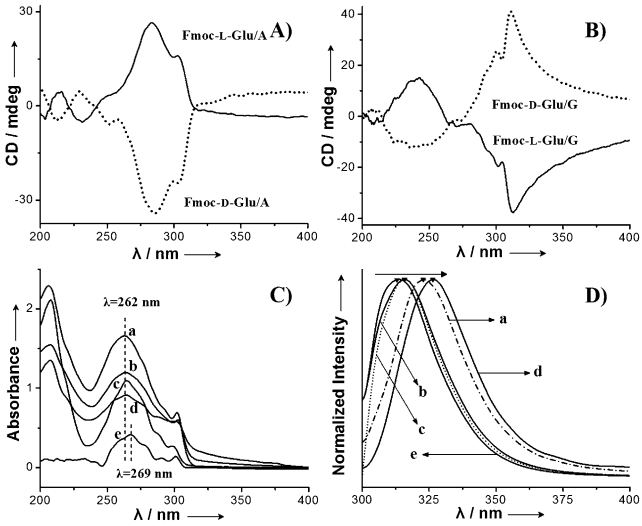

Figure 2. A) CD spectra of the hydrogels of Fmoc-L(D)-Glu/A. B) CD spectra of Fmoc-L(D)-Glu/G. C, D) UV/Vis and fluorescence spectra of samples (the line of a b c d represents the co-assembly of Fmoc-Glu with four nucleobases:A, T, C, G, respectively. Curve e represents native Fmoc-Glu.

The CD signal of the Fmoc-Glu suspension is almost silent in the range of 250 nm–350 nm, ascribed to the Fmoc chromophores, even though Fmoc-Glu is a chiral molecule.[3c,8] This result indicates that the molecular chirality could not be transferred to Fmoc chromophores or amplified to be detected in the CD spectra. When Fmoc-Glu co-assembled with A or G, obvious CD signals were obtained (Figure 2). Fmoc-L-Glu/A showed characteristic Cotton effects in the region of 270–310 nm (Figure 2 A), which are consistent with the adsorption band in the region of 270–350 nm, assigned to the π-π* transitions of the Fmoc moiety[9] (Figure 2 C). In the case of the D-enantiomer of Fmoc-Glu with A, the mirror image of the CD spectrum profile with that

of Fmoc-L-Glu/A was obtained, indicating that A induces chiral packing of Fmoc-Glu. Additionally, the contribution of possible linear dichroism (LD) on the CD signals were evaluated.[10] As shown in Figure S5, the LD signal was much lower than that of the CD signal, indicating that the LD is negligible in our system. As for Fmoc-L-Glu/G (Figure 2B), the CD spectrum profile exhibits small differences from that of Fmoc-Glu/A. First, there are two negative Cotton effects located at 301 and 311 nm, which show red-shift relative to Fmoc-Glu/A. Considering the white gel formed in Fmoc-Glu/G, we speculate the red-shift of the CD signals is the result of chiral scattering. But it is worth noting that the hydrogel containing A exhibits an opposite CD signal to the hydrogel with G: Fmoc-L-Glu shows positive CD signals when it interact with A, however, Fmoc-L-Glu presents a negative Cotton effect when it co-assembles with G. The D-enantiomer of Fmoc-Glu shows an opposite CD signal when it co-assembles with A or G, respectively. We speculate the angle of the Fmoc moiety packing is different when Fmoc-Glu co-assemble with A or G, respectively. In comparison with that of A or G, complexes of Fmoc-Glu/C did not exhibit obvious CD signals (Figure S4). Although Fmoc-Glu/T showed CD signals, it did not exhibit obvious helical nanostructures. This indicates that A and G induced more effective expression of helicity in the assemblies than T and C.

The fluorescence spectra of Fmoc-Glu with four nucleobases are shown in Figure 2D. In comparison with plain Fmoc-Glu, A and G cause a red-shift in the fluorescence emission, while T and C almost maintain the Fmoc-Glu emission, indicating that in the Fmoc-Glu/A (G) system, π-π stacking is stronger than that of the T (C) system. This stronger π-π stacking is related to the purine structures and may finally lead to the hydrogel formation.[3c,e]

Furthermore, these helical structures are found to be able to transfer their chirality to a second achiral component. Thioflavin T (ThT), as the most popular fluorescent probe, is used for the detection of amyloid fibers and also to study gel formation, due to its environment-dependent emission behavior.[11] It is reported that the fluorescence of ThT increases remarkably when it is bound to amyloid fibers or other hydrophobic patches because its freely rotating aromatic rings become fixed.[12] In this context, ThT was selected as an indicator to investigate whether the chiral sense of the helix in Fmoc-Glu/A (G) transferred to the achiral moiety.

Purine A (adenine) could co-assemble with Fmoc-Glu into a semi-transparent hydrogel (Figure 3a, left) and has no obvious fluorescence under the irradiation (Figure 3b, left). When ThT was added in Fmoc-Glu/A gel, a semi-transparent yellow hydrogel formed, and this hydrogel emitted cyan fluorescence (Figure 3b, middle). It is clear that no hydrogel is formed when adenine is absent, and there is no fluorescence emission, indicating that the hydrogel media and the nucleobase play a significant role in fluorescence emission. Different amounts of ThT were doped into the complex of Fmoc-Glu/A to study the effect of ThT concentration on hydrogel properties. The results reveal that ThT did not affect the formation of hydrogel until its concentration reached 0.2 mM (Figure S6a). Additionally, the fluorescence intensity gradually increases with increasing concentrations of ThT, and

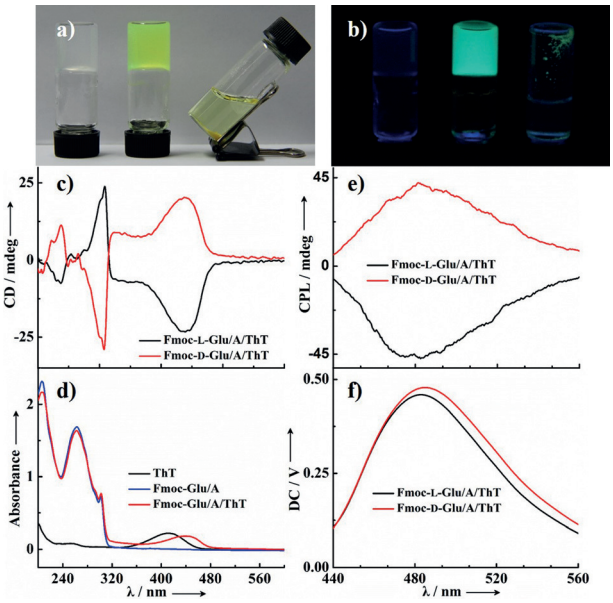

Figure 3. Photo images of assemblies containing Fmoc-Glu under visible light (a) and UV light irradiation (b): from left to right: Fmoc-Glu/A, Fmoc-Glu/A/ThT, Fmoc-Glu/ThT; c, d) CD and UV/Vis spectra of the hydrogels composed of Fmoc-L(D)-Glu/A/ThT, respectively; e, f) CPL spectra of Fmoc-L(D)-Glu/A/ThT.

a maximal value was obtained at 0.1 mM (Figure S6b). Afterwards, the fluorescent quantum yields were obtained in a calibrated integrated sphere under the photoluminescence (PL) curve in the wavelength range 430–630 nm, and the result (Φ_χ) was about 45%. Thus, we selected 0.1 mM ThT for the following studies.

The effect of ThT on the nanostructures of Fmoc-Glu/A hydrogels was also investigated by AFM and SEM techniques. Upon addition of ThT, the helical sense of the nanostructures was preserved, and more, the helical pitch and width of the helix increased simultaneously (Figures 1c,d and S7). SEM images revealed that no phase separation was observed, indicating that ThT could insert into helical nanostructures (Figure S7a,b). Detailed analysis of the AFM images (Figure S7c–j) showed that the pitch of the helix is larger than that of Fmoc-L-Glu/A. The left-handed helix with helical pitch is about 125 nm for Fmoc-L-Glu/A; upon addition of ThT, the helical pitch increases to about 145 nm. Moreover, the helix width increases from 90 ± 20 nm to about 130 ± 20 nm upon addition of ThT. The increase of helical pitch and width further supports ThT being inserted into the helix. Furthermore, rheological studies provide further evidence for ThT insertion into fibers formed by Fmoc-Glu/A. Figure S8 confirmed that small amount of ThT make the hydrogel stiffer and more solid. Dynamic frequency sweep experiments on the hydrogels of Fmoc-Glu/A and Fmoc-Glu/A/ThT show that hydrogels containing ThT exhibited higher storage moduli and loss moduli (Figure S8a). Addition of ThT increased the yield strain[13] (Figure S8b, taken as the point at which $G'' > G'$) of the hydrogel. Both G' and G'' are much higher for the ThT-containing sample. These data strongly suggest that the mechanical properties of the hydrogels would

be enhanced by addition of ThT, indicating ThT joined in the co-assembly with Fmoc-Glu and A.

The CD spectra were also recorded to monitor the chiral properties of the achiral ThT-doped hydrogel (Figure 3). As for Fmoc-L-Glu/A/ThT, besides a Cotton effect at about 301 nm, which belonged to helical packing of Fmoc chromophores, a new negative CD signal appeared at 442 nm (Figure 3c). This new CD signal could be ascribed to ThT chromophores, which is consistent with the absorption band (Figure 3d), indicating that chirality of ThT is induced in the matrix of the helix formed by Fmoc-Glu and A.[14] To further verify the effectiveness of chirality transfer, we employed the enantiomer (Fmoc-D-Glu) to repeat the experiments, and exact mirror CD signals with substantial characteristic Cotton effects (CEs) were found, which supports our analysis. In addition, to confirm that the purine A plays an indispensable role in realizing the chirality transfer, the CD spectrum of Fmoc-Glu/ThT was monitored. The CD signal for ThT chromophore was found to be silent without A (Figure S9a). We also tested the hydrogel containing another purine (G) to induce the chirality of ThT (Figure S9b). As for Fmoc-L-Glu/G, a negative Cotton effect was observed at the ThT adsorption band, which is the same as in Fmoc-L-Glu/A, although A and G cause opposite CD signals in the Fmoc chromophores. All of these results indicate that ThT follows the chirality of Fmoc-Glu and the purine base functions as a bridge to transfer the chirality of Fmoc-Glu to ThT. With the increasing interest in developing materials exhibiting circularly polarized luminescence (CPL),[15] supramolecular gels with CPL emission, as functional soft materials, have been explored recently. We further monitored the CPL spectra of hydrogels containing ThT. It was exciting to find that a wide negative peak centered at 490 nm exhibited in the Fmoc-L-Glu/A/ThT hydrogels, whereas a mirror CPL signal appeared in Fmoc-D-Glu/A/ThT hydrogels (Figure 3e,f). The λ_{max} of the CPL signal is consistent with the fluorescence emission spectra, and the $|g_{em}|$ values for Fmoc-L(D)-Glu/A/ThT were $\approx 7.17 \times 10^{-3}$ and 6.22×10^{-3}, respectively. The CPL emission was also found in the hydrogel of Fmoc-Glu/G/ThT (Figure S9c). For pyrimidine base (T), there is no induced CD and CPL signals for doped ThT (Figure S9d,e), further suggesting that π-π stacking between the purine base and ThT lead to the chirality transfer.

X-ray diffraction (XRD) patterns were obtained for the purine-triggered Fmoc-Glu gels and ThT-inserted gels. Well-defined XRD patterns of Fmoc-Glu itself display d-spacing of 2.36, 1.20, 0.80, 0.61, 0.48, and 0.40 nm, calculated from Bragg's equation, which corresponds to ratio of 1, 1:2, 1:3, 1:4, 1:5 and 1:6, respectively, indicating an obvious lamellar structure with a d-spacing of 2.36 nm[16] (Figure 4a). This d-spacing is larger than one molecular length of Fmoc-Glu (1.34 nm) but shorter than two, indicating a bilayer structure of Fmoc-Glu with an overlapping Fmoc moiety. It was found that the XRD patterns do not change significantly after assembly with the nucleobase. In contrast, we changed the mixing ratio of Fmoc-Glu to A and investigated their gel formation (Figure S1), nanostructures (Figure S10), and CD spectra (Figure S11), and found that only in the ratio of 2:1, Fmoc-Glu and A formed the stable hydrogel and uniform

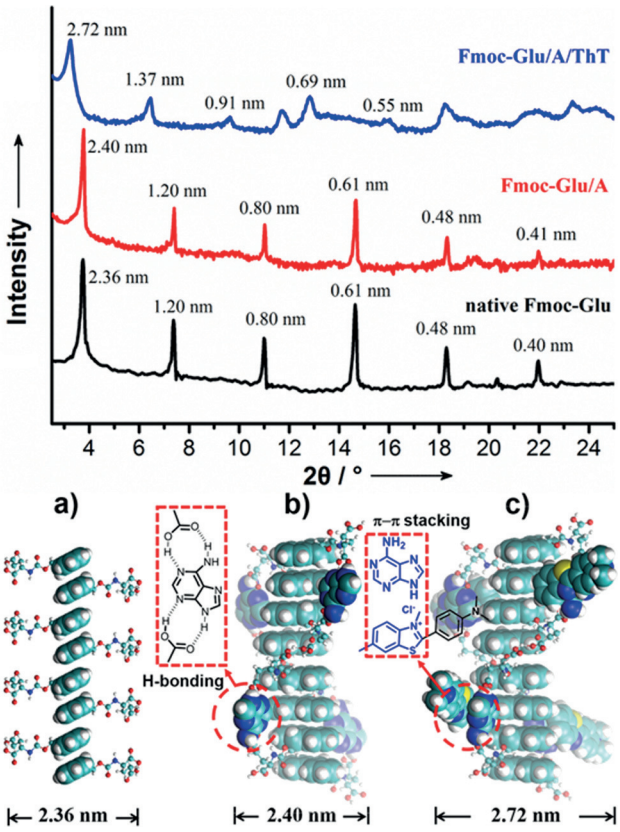

Figure 4. Top: XRD patterns of assemblies of Fmoc-Glu, Fmoc-Glu/A, and Fmoc-Glu/A/ThT. Bottom: illustration of molecular packing. Front view of a) Fmoc-Glu packing as a bilayer structure with π-π stacking of Fmoc moiety; b) purine base, A, inserted into two alternate glutamic acid molecules through hydrogen bonding between A and carboxylic acid; c) ThT molecules inserted into the Fmoc-Glu/A complex by π-π stacking with A. For simplicity, only one pair of lamellar structure is shown.

helical fibers. Based on these results, we speculate that the nucleobase laterally attached on the bilayer surface of Fmoc-Glu (Figure 4b). The purine bases interact with two alternate glutamic acids through hydrogen bonding[17] (Figure 4b, inset), and the bulky purine base may cause the torsion of neighboring Fmoc-Glu molecules. This purine-base-inserted bilayer structure serves as a basic repeat unit, which forms multiple bilayers, and further hierarchically self-assembles into higher level nanohelices. The larger conjugated structure of purine nucleobases than that of pyrimidines is attributed to stronger π-π stacking, causing the formation of hydrogels and chiral structures. After inserting ThT, the d-spacing is a slightly enlarged (2.72 nm), and the increment (0.32 nm) may be ascribed to the length of the dimethylbenzenamine moiety. The benzothiazole moiety is inserted into the bilayer to cause the helical pitch to increase further (Figure 4c).

Fmoc-Glu was found to co-assemble into hydrogels with purine nucleobases, and helical architectures were exhibited in hydrogels. In contrast, pyrimidine nucleobases cannot trigger Fmoc-Glu either into chiral structures or hydrogels. It was suggested that the hydrogen bonding between the A or G and glutamic acid, enhanced π-π stacking, and hydrophobic interaction of the two-component assemblies synergetic

contributed to the expression of chiral nanostructures. Further, the helical structures worked as a matrix and transferred the chirality to a fluorescent dye ThT. In this system, the achiral nucleobase acted as a bridge to mediate chirality transfer from Fmoc-Glu to ThT. By combination of chirality transfer and fluorescence, a hydrogel emitting CPL was obtained. The results demonstrated that the achiral nucleobase plays an essential role in chiral self-assembly.

Acknowledgments

This work was supported by the Basic Research Development Program (2013CB834504) the National Natural Science Foundation of China (Nos 21473219 and 91427302), and the Strategic Priority Research Program of the Chinese Academy of Sciences (XDB12020200).

Keywords: chirality transfer · circular polarized fluorescence · helical structures · nucleobases · purines

How to cite: *Angew. Chem. Int. Ed.* **2016**, *55*, 15062–15066
Angew. Chem. **2016**, *128*, 15286–15290

[1] a) Y. Timsit, *Int. J. Mol. Sci.* **2013**, *14*, 8252–8270; b) R. P. Cheng, S. H. Gellman, W. F. DeGrado, *Chem. Rev.* **2001**, *101*, 3219–3232.

[2] a) P. Zhou, R. Shi, J. Yao, C. Sheng, H. Li, *Coord. Chem. Rev.* **2015**, *292*, 107–143; b) Y. Gao, J. Hao, J. Wu, X. Zhang, J. Hu, Y. Ju, *Nanoscale* **2015**, *7*, 13568–13575; c) M. Liu, L. Zhang, T. Wang, *Chem. Rev.* **2015**, *115*, 7304–7397; d) T. G. Barclay, K. Constantopoulos, J. Matisons, *Chem. Rev.* **2014**, *114*, 10217–10291; e) B. Liu, Y. Cao, Z. Huang, Y. Duan, S. Che, *Adv. Mater.* **2015**, *27*, 479–497; f) A. Saha, J. Adamcik, S. Bolisetty, S. Handschin, R. Mezzenga, *Angew. Chem. Int. Ed.* **2015**, *54*, 5408–5412; *Angew. Chem.* **2015**, *127*, 5498–5502; g) S. Sivakova, S. J. Rowan, *Chem. Soc. Rev.* **2005**, *34*, 9–21; h) A. Bertolani, L. Pirrie, L. Stefan, N. Houbenov, J. S. Haataja, L. Catalano, G. Terraneo, G. Giancane, L. Valli, R. Milani, O. Ikkala, G. Resnati, P. Metrangolo, *Nat. Commun.* **2015**, *6*, 7574, DOI: 10.1038/ncomms8574.

[3] a) M. B. Avinash, T. Govindaraju, *Nanoscale* **2014**, *6*, 13348–13369; b) A. Nuthanakanti, S. G. Srivatsan, *Nanoscale* **2016**, *8*, 3607–3619; c) A. M. Smith, R. J. Williams, C. Tang, P. Coppo, R. F. Collins, M. L. Turner, A. Saiani, R. V. Ulijn, *Adv. Mater.* **2008**, *20*, 37–41; d) V. Jayawarna, S. M. Richardson, A. R. Hirst, N. W. Hodson, A. Saiani, J. E. Gough, R. V. Ulijn, *Acta Biomater.* **2009**, *5*, 934–943; e) S. Fleming, S. Debnath, P. W. J. M. Frederix, T. Tuttle, R. V. Ulijn, *Chem. Commun.* **2013**, *49*, 10587–10589; f) Y. Wang, W. Qi, R. Huang, X. Yang, M. Wang, R. Su, Z. He, *J. Am. Chem. Soc.* **2015**, *137*, 7869–7880; g) B. Adhikari, J. Nanda, A. Banerjee, *Soft Matter* **2011**, *7*, 8913–8922; h) D. M. Ryan, S. B. Anderson, B. L. Nilsson, *Soft Matter* **2010**, *6*, 3220–3231; i) H. H. Saito, M. Suzuki, K. Hanabusa, *Langmuir* **2009**, *25*, 8579–8585; j) J. Ren, Y. Hu, C. Lu, W. Guo, M. A. Aleman-Garcia, F. Ricci, I. Willner, *Chem. Sci.* **2015**, *6*, 4190–4195; k) J. H. Jung, G. John, M. Masuda, K. Yoshida, S. Shinkai, T. Shimizu, *Langmuir* **2001**, *17*, 7229–7232.

[4] a) G. Liu, L. Zhu, W. Ji, C. Feng, Z. Wei, *Angew. Chem. Int. Ed.* **2016**, *55*, 2411–2415; *Angew. Chem.* **2016**, *128*, 2457–2461; b) X. Zhu, P. Duan, L. Zhang, M. Liu, *Chem. Eur. J.* **2011**, *17*, 3429–3437.

[5] M. O. M. Piepenbrock, N. Clarke, J. W. Steed, *Langmuir* **2009**, *25*, 8451–8456.

[6] a) I. Usov, R. Mezzenga, *Macromolecules* **2015**, *48*, 1269–1280; b) J. Adamcik, J. Jung, J. Flakowski, P. D. L. Rios, G. Dietler, R. Mezzenga, *Nat. Nanotechnol.* **2010**, *5*, 423–428; c) S. Assenza, J. Adamcik, R. Mezzenga, P. D. L. Rios, *Phys. Rev. Lett.* **2014**, *113*, 268103.

[7] I. Danila, F. Riobe, F. Piron, J. Puigmarti-Luis, J. D. Wallis, M. Linares, H. Agren, D. Beljonne, D. B. Amabilino, N. Avarvari, *J. Am. Chem. Soc.* **2011**, *133*, 8344–8353.

[8] a) N. Zanna, A. Merlettini, G. Tatulli, L. Milli, M. L. Focarete, C. Tomasini, *Langmuir* **2015**, *31*, 12240–12250; b) P. Xing, X. Chu, M. Ma, S. Li, A. Hao, *Chem. Asian J.* **2014**, *9*, 3440–3450; c) D. M. Ryan, T. M. Doran, B. L. Nilsson, *Langmuir* **2011**, *27*, 11145–11156.

[9] a) S. Yagai, M. Yamauchi, A. Kobayashi, T. Karatsu, A. Kitamura, T. Ohba, Y. Kikkawa, *J. Am. Chem. Soc.* **2012**, *134*, 18205–18208; b) M. Yamauchi, T. Ohba, T. Karatsu, S. Yagai, *Nat. Commun.* **2015**, *6*, 8936.

[10] a) K. Tsuda, Md. A. Alam, T. Harada, T. Yamaguchi, N. Shii, T. Aida, *Angew. Chem. Int. Ed.* **2007**, *46*, 8198–8202; *Angew. Chem.* **2007**, *119*, 8346–8350; b) M. Wolffs, S. J. George, Ž. Tomović, S. C. J. Meskers, A. P. H. J. Schenning, E. W. Meijer, *Angew. Chem. Int. Ed.* **2007**, *46*, 8203–8205; *Angew. Chem.* **2007**, *119*, 8351–8353.

[11] a) N. Nespovitaya, J. Gath, K. Barylyuk, C. Seuring, B. H. Meier, R. Riek, *J. Am. Chem. Soc.* **2016**, *138*, 846–856; b) S. Xu, Q. Li, J. Xiang, Q. Yang, H. Sun, A. Guan, L. Wang, Y. Liu, L. Yu, Y. Shi, H. Chen, Y. Tang, *Sci. Rep.* **2016**, *6*, 24793.

[12] G. M. Peters, L. P. Skala, J. T. Davis, *J. Am. Chem. Soc.* **2016**, *138*, 134–139.

[13] M. O. M. Piepenbrock, N. Clarke, J. W. Steed, *Soft Matter* **2011**, *7*, 2412–2418.

[14] P. Duan, H. Cao, L. Zhang, M. Liu, *Soft Matter* **2014**, *10*, 5428–5448.

[15] J. Mohanty, N. Barooah, V. Dhamodharan, S. Harikrishna, P. I. Pradeepkumar, A. C. Bhasikuttan, *J. Am. Chem. Soc.* **2013**, *135*, 367–376.

[16] I. W. Hamley, V. Castelletto, *Prog. Polym. Sci.* **2004**, *29*, 909–948.

[17] a) L. J. Thompson, N. Elias, L. Male, M. Tremayne, *Cryst. Growth Des.* **2013**, *13*, 1464–1472; b) C. McHugh, A. Erxleben, *Cryst. Growth Des.* **2011**, *11*, 5096–5104.

Received: September 4, 2016
Revised: October 5, 2016
Published online: November 3, 2016

